Generalized Moment Expansion for the Mössbauer Spectrum of Brownian Particles

Walter Nadler and Klaus Schulten
Physik-Department der Technischen Universität München, 8046 Garching, Federal Republic of Germany, and Max-Planck-Institut für Biophysikalische Chemie, 3400 Göttingen, Federal Republic of Germany
(Received 9 June 1983)

An algorithm is suggested for the Mössbauer spectrum $I(\omega)$ of an atom undergoing one-dimensional Brownian motion in an arbitrary potential. The algorithm reproduces simultaneously the low- and high-frequency dependence of $I(\omega)$ to a desired accuracy.

PACS numbers: 87.15.By, 76.80.+y

The structural analysis of proteins by nonresonant x-ray scattering has contributed much to biology. In recent years the accuracy of the scattering data has been enhanced to a degree which revealed that proteins do not exist in single conformations but rather exhibit innate temperature-dependent conformational distributions.[1] These distributions show a relationship to the functional states of proteins. Since nonresonant scattering probes particles on a time scale short compared to atomic motion, the scattering intensity does not provide information on the dynamics connected with conformational transitions. In fact, the scattering intensity for classical particles is given by the Debye-Waller factor

$$f_{\mathrm{DW}} = |\langle \exp(i\vec{k}\cdot\vec{x})\rangle_T|^2, \tag{1}$$

where $\vec{k}$ is the scattering vector and $\langle\cdots\rangle_T$ denotes the thermal average. A welcome extension in this respect is provided by the resonant scattering of γ rays at Mössbauer atoms.[2,3] The line shape of the Mössbauer transition yields information on the motion of the atom during the lifetime Γ^{-1} of the metastable state. For an analysis the observed line-shape function $I(\omega)$ is usually expanded in accordance with the accuracy of the data in terms of two or three Lorentzians,[2,3]

$$I(\omega) = \frac{\sigma_0\Gamma}{2}\,\mathrm{Re}\left(\sum_{n=0}^{2}\frac{f_n}{i\omega+\Gamma_n}\right). \tag{2}$$

The resulting intensities f_n and linewidths Γ_n ($\Gamma_0 = \Gamma/2$) are then investigated in terms of models of the stochastic dynamics assumed for the atom.

The Mössbauer spectral analysis outlined has been carried out for a number of proteins containing ^{57}Fe at their functional site.[2,3] The temperature dependence of the Mössbauer data revealed a sudden transition from a confined motion at low temperatures to a less confined motion at high temperatures, the transition being characteristic of the protein and its surroundings. It is, of course, most desirable to understand this behavior. Unfortunately, the theoretical analysis of Mössbauer spectra has been hampered by the inability of previous methods to determine line shapes for anything but the most simple models, i.e., jumps on equivalent lattice sites,[4,5] and Brownian motion in constant and in harmonic potentials.[6,7] Further progress in the understanding of available Mössbauer spectra requires necessarily a description for potentials which account better for the complex interactions in proteins. According to the investigations of Frauenfelder, Petsko, and Tsernoglu,[1] and Austin *et al.*,[8] such potentials are of the multistable type. In this Letter we introduce an algorithm which yields for one-dimensional Brownian motion Mössbauer line shapes for essentially arbitrary static potentials. For a demonstration the algorithm will be applied to a bistable potential.

In the case of ^{57}Fe resonant scattering the accuracy of the observed line-shape function (2) is significant only for frequencies between one and one hundred natural linewidths Γ ($\Gamma = 7\times10^6\ \mathrm{s}^{-1}$), i.e., the observations probe the stochastic motion of ^{57}Fe for times between 1 ns and about 100 ns. One can consider the motion of the atom as classical, influenced by thermal noise and friction. In fact, one can safely expect in a dense matrix like a protein that the motion is in the strong-friction limit. If we assume the magnitude of the thermal noise to increase linearly with temperature,[9] the fluctuation-dissipation theorem dictates a temperature-dependent diffusion coefficient $D = D_0 T$. The spatial resolution of the observation by ^{57}Fe Mössbauer spectroscopy is determined by the momentum $k = 7.3\ \text{Å}^{-1}$ of the γ quantum and measures about 0.1 Å. The dominant relaxation frequencies for Brownian processes on this length scale have values of about k^2D. In proteins this frequency value should be much larger than $1\ \mathrm{ns}^{-1}$. In fact, molecular-dynamics simulations[10] show that local (0.1 Å) relaxation occurs within 10 ps. Hence, only the slow fraction of Brownian processes, e.g., barrier cross-

ings, will contribute to the observed Mössbauer spectrum. This is the key ideal of the following treatment. Contrary to conventional moment expansions which reproduce well the short-time response of systems and include long-time effects by "memory functions" for which no systematic alogrithm exists, we will describe here the line shape $I(\omega)$ in a more balanced way, simultaneously reproducing the short-time (high-frequency) as well as the long-time (low-frequency) behavior adequately.

The Mössbauer line-shape function $I(\omega)$ is given by[11]

$$I(\omega)=(\sigma_0\Gamma/2)\mathrm{Re}[\sigma(\omega)], \tag{3}$$

$$\sigma(\omega)=\int dx\exp(ikx)[i\omega-L(x)+\Gamma/2]^{-1}\times\exp(-ikx)p_0(x), \tag{4}$$

where σ_0 is the resonance absorption cross section,

$$L(x)=\partial_x D[\partial_x+\beta U'(x)] \tag{5}$$

the Fokker-Planck operator describing the Brownian motion in a potential $U(x)$ with diffusion coefficient $D=D_0T$, and $p_0(x)$ the initial Boltzmann distribution of the scattering atom, i.e., $p_0(x)\sim\exp[-\beta U(x)]$. A spectral expansion of $\sigma(\omega)$ yields

$$\sigma(\omega)=\sum_{n=0}(i\omega-\lambda_n+\Gamma/2)^{-1}|\psi_n(k)|^2, \tag{6}$$

where $\lambda_n\leq 0$ are the eigenvalues and $\psi_n(k)$ the Fourier-transformed nonorthogonal eigenfunctions of $L(x)$. In the case of a harmonic potential[12] one derives $\lambda_n=-nD/\langle x^2\rangle_T$ and

$$|\psi_n(k)|^2=\exp(-k^2\langle x^2\rangle_T)(k^2\langle x^2\rangle_T)^n/n!.$$

This exact result will be used to test the suggested algorithm below.

The proposed algorithm starts from the observation that the high- and low-frequency expansions

$$\sigma(\omega)\underset{\omega\to\infty}{\sim}\frac{1}{i\omega}\sum_{n=0}^{\infty}\mu_n\left(-\frac{1}{i\omega}\right)^n,\qquad \sigma(\omega)\underset{\omega\to 0}{\sim}\sum_{n=0}^{\infty}\mu_{-n-1}(-i\omega)^n, \tag{7}$$

can actually be constructed for arbitrary potentials $U(x)$ since the coefficients *(generalized moments)*

$$\mu_n=(-1)^n\int dx\exp(ikx)[L(x)-\Gamma/2]^n\times\exp(-ikx)p_0(x) \tag{8}$$

can be evaluated for *positive* as well as for *negative* n. The evaluation is straightforward for positive n. For negative indices one can discretize the differential operator $L(x)$ fixing $x=x_1, x_2, \ldots$, and employ a well-known recursive algorithm[13] for the inverse of the resulting tridiagonal matrix L. The computational effort of the recursive scheme grows only linearly with the number of x_i's chosen. It can therefore easily be applied to dimensions of a few thousand. Below a certain mesh size the μ_n, $n<0$, have been found independent of the discretization scheme. The μ_n can, hence, be constructed to include any desired feature of model potential surfaces.

In accordance with the analysis (2) of the experimental data one seeks an approximate $s(\omega)\simeq\sigma(\omega)$ of the type

$$s(\omega)=\sum_{n=0}^{N-1}f_n/(i\omega+\Gamma_n). \tag{9}$$

One can show that if the amplitudes and linewidths obey

$$\sum_{n=0}^{N-1}f_n\Gamma_n{}^m=\mu_m,\quad m=-N_l,-N_l+1,\ldots,N_h-1,\qquad 2N=N_l+N_h, \tag{10}$$

then $s(\omega)$ reproduces the ω dependence of expansions (7) for the coefficients μ_n, $-N_l\leq n\leq N_h-1$. For $N\leq 3$ Eqs. (10) can be solved algebraically; for $N>3$ one should resort to a representation in terms of an eigenvalue problem.[14]

In Fig. 1 we compare for the case of a Brownian motion in a harmonic potential approximate line-shape functions with the exact solution. For the parameters chosen the exact expansion (6) must sum at least ten lines in order to converge within 1% error. A termination after the third term would yield a poor approximation. On the other hand, the approximate line-shape function yields an accurate description of the central part of the line, i.e., that part on which any analysis of spectral data currently hinges, with only three Lorentzians reproducing the moments μ_{-5} to μ_0 of the exact $I(\omega)$. The comparison reveals that the approximation should take into account the low-frequency moments $\mu_{-1}, \mu_{-2}, \ldots$, rather than the high-frequency moments $\mu_1, \mu_2, \ldots$. The moment μ_0 carries the total intensity of $I(\omega)$. Since only a small number of moments have to be considered the algorithm proposed does not depend sensitively on the numerical accuracy of the moments as would be the case if more extended expansions would be required. Incidently, the de-

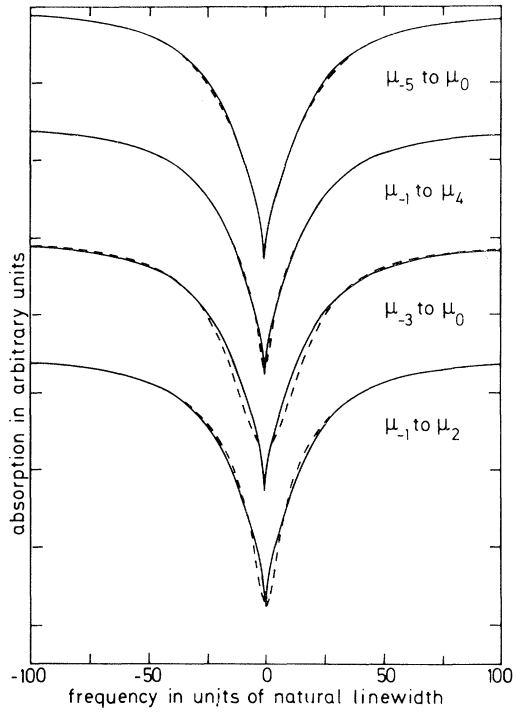

FIG. 1. Comparison of Mössbauer line shapes for Brownian motion in a harmonic oscillator ($D=3\times10^6$ Å^2/s, $\langle x^2\rangle_T=0.1$ Å^2) resulting from an exact (see text) calculation (solid line) and from generalized-moment expansions (dashed line).

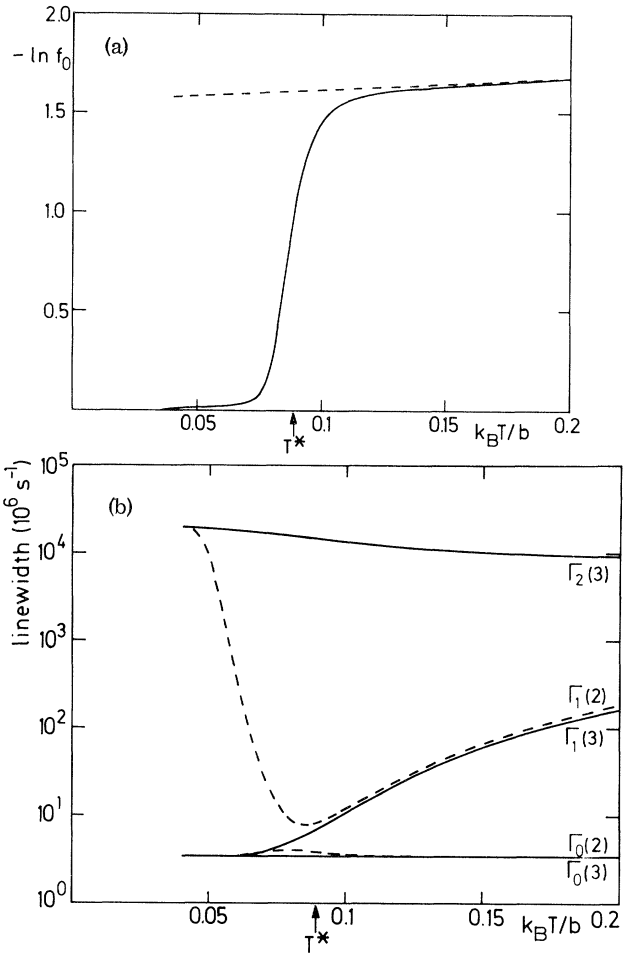

FIG. 2. Temperature dependence of the Mössbauer line-shape characteristics for a Brownian particle in a bistable well as given in the text ($D=100k_BT/b$ Å^2/s, $x_0=0.3$ Å). (a) Lamb-Mössbauer factor f_0 (solid line) of the two-Lorentzian-line (μ_{-3} to μ_0) representation and Debye-Waller factor f_{DW} from (1) (dashed line). (b) Line widths resulting from a two-Lorentzian-line representation (dashed line) and a three-Lorentzian-line (μ_{-5} to μ_0) representation (solid line).

scription which reproduces only the coefficients μ_{-1} and μ_0 of (7) is equivalent to the "first passage time" approximation usually applied to reaction-diffusion processes.[15] Reference 15 already introduces a generalization of the first-passage-time approximation which reproduces the moments μ_1, μ_0, μ_{-1}, and μ_{-2}.

The comparison in Fig. 1 also demonstrates the important feature of the suggested algorithm which is that only a few moments are needed in the construction of an approximate $I(\omega)$. In particular, for situations when direct comparison with experimental data is a concern, the requirement of the algorithm can be tailored to the accuracy of the data available. For example, current Mössbauer spectra are appropriately fitted by two or three Lorentzians.

As a nontrivial application of the algorithm presented we consider the Mössbauer transition for an atom diffusing in the bistable potential well $U(x)=-b\exp[-\cos^2(\pi x/x_0)]$, $-x_0\leq x\leq x_0$. Figure 2 presents the temperature dependence of the intensity f_0 of the natural line, the so-called Lamb-Mössbauer factor, and the line widths Γ_0, Γ_1 (and Γ_2) of a two (three) Lorentzian line representation. The algorithm is based on the generalized moments μ_{-3} to μ_0 (μ_{-5} to μ_0). Figure 2(a) demonstrates that at a temperature T^* the Lamb-Mössbauer factor exhibits a sudden drop to approach the Debye-Waller factor (1) at high temperatures. This behavior can be understood qualitatively by inspecting expansion (6). In the case of the bistable potential at low temperatures several eigenvalues are in the range of $-\Gamma/2$ and, therefore, contribute to the "natural" line, whereas at high temperatures this is not the case. The

three-line representation yields $\Gamma_0(3)$ identical to the natural linewidth $\Gamma/2$. The linewidth $\Gamma_1(3)$ splits off from $\Gamma_0(3)$ at T^*. This line originates from jumps between the two potential wells above the temperature T^*. This interpretation is corroborated by the fact that $\Gamma_1(3)$ coincides with the value of $\Gamma/2+1/\tau(T)$, where $\tau(T)$ is the mean first passage time between the wells,[15]

$$\tau(T)=2\int_{-x_0}^{0} dx[Dp_0(x)]^{-1}\left[\int_{-x_0}^{x} dy\, p_0(y)\right]^2. \quad (11)$$

This result identifies the transition temperature T^* as the temperature at which $\tau(T)$ equals $2/\Gamma$. Obviously only at this temperature can the resonant scattering process begin to detect the interwell transitions. The third linewidth $\Gamma_2(3)$ is actually due to relaxation processes in one well as this width is also found in a two-line spectrum of a single potential well. Figure 2(b) demonstrates the behavior of the two-line representation. This representation reproduces accurately the contribution of the natural line as described by the three-line representation and around temperature T^* interpolates between the large third linewidth $\Gamma_2(3)$ and the emerging second linewidth $\Gamma_1(3)$.

In the case of more complicated potentials a description in terms of more than three lines may be necessary. For example in a multistable potential with M minima, $M+1$ lines provide an accurate description.[16] In this case, $\Gamma_0(M+1)=\Gamma/2$ holds. However, if the accuracy of spectral data is not sufficient to fit more than three Lorentzians, one may wish, in accordance with the quality of the available data, to limit the algorithm to only three lines as well. In such a case one may determine for example $\Gamma_0(3)>\Gamma/2$ indicating that lines with widths close to that of the natural line are not resolved.

However, the algorithm prevents one also from choosing too many lines. For example, if one considers $I(\omega)$ for a freely diffusing Mössbauer atom an exact calculation yields a single Lorentzian of width $\Gamma/2+k^2D$. Application of our algorithm yields the exact Lorentzian in a one-line-fit approach. An attempt to fit more lines fails since in this case Eqs. (10) are ill conditioned.

The authors would like to thank A. Brünger, Z. Schulten, and F. Parak for inspiring and helpful discussions. This work has been supported by the Deutsche Forschungsgemeinschaft (SFB-143C1).

[1]H. Frauenfelder, G. A. Petsko, and D. Tsernoglu, Nature (London) 280, 558 (1979).

[2]F. Parak, E. W. Knapp, and D. Kucheida, J. Mol. Biol. 161, 177 (1982).

[3]E. R. Bauminger *et al.*, Proc. Natl. Acad. Sci. U.S.A. 79, 4967 (1982).

[4]A. Bläsius, R. S. Preston, and U. Gonser, Z. Phys. Chem. (Leipzig) NF115, 187 (1979).

[5]F. Parak *et al.*, J. Mol. Biol. 145, 825 (1981).

[6]I. Nowik *et al.*, Phys. Rev. Lett. 50, 1528 (1983).

[7]E. W. Knapp, S. Fischer, and F. Parak, J. Phys. Chem. 86, 5042 (1982), and J. Chem. Phys. 78, 4701 (1983).

[8]R. H. Austin *et al.*, Biochemistry 14, 5355 (1975).

[9]H. Haken, *Synergetics* (Springer, Berlin, 1977), Chap. 6.

[10]J. A. McCammon, B. R. Gelin, and M. Karplus, Nature (London) 267, 555 (1977).

[11]K. S. Singwi and A. Sjölander, Phys. Rev. 120, 1093 (1960), Eq. (5); noting that in the case of classical stochastic motion $G(x,t)$ is the solution of $\partial_t G(x,t)=L(x)G(x,t)$ and averaging over initial conditions yields our Eqs. (3) and (4).

[12]K. Schulten, Z. Schulten, and A. Szabo, Physica (Utrecht) 100A, 599 (1980).

[13]The Gaussian elimination procedure is described in many textbooks on applied mathematics; e.g., B. Noble, *Applied Linear Algebra* (Prentice-Hall, Englewood Cliffs, 1969).

[14]A. Brünger, thesis, Technische Universität München, March 1982 (unpublished).

[15]K. Schulten, Z. Schulten, and A. Szabo, J. Chem. Phys. 74, 4426 (1981).

[16]W. Nadler and K. Schulten, to be published.